doi:10.1016/j.jmb.2012.05.004 J. Mol. Biol. (2012) 422, 183–191

Contents lists available at www.sciencedirect.com

Journal of Molecular Biology

journal homepage: http://ees.elsevier.com.jmb

COMMUNICATION

Role of MINOS in Mitochondrial Membrane Architecture: Cristae Morphology and Outer Membrane Interactions Differentially Depend on Mitofilin Domains

Ralf M. Zerbes[1,2]†, Maria Bohnert[1,2]†, David A. Stroud[1], Karina von der Malsburg[1], Anita Kram[3], Silke Oeljeklaus[2,4,5], Bettina Warscheid[2,4,5], Thomas Becker[1,5], Nils Wiedemann[1,5], Marten Veenhuis[3], Ida J. van der Klei[3], Nikolaus Pfanner[1,5]* and Martin van der Laan[1,5]*

[1]*Institut für Biochemie und Molekularbiologie, ZBMZ, Universität Freiburg, 79104 Freiburg, Germany*
[2]*Fakultät für Biologie, Universität Freiburg, 79104 Freiburg, Germany*
[3]*Groningen Biomolecular and Biotechnology Institute, University of Groningen, Kluyver Centre for Genomics of Industrial Fermentation, 9700 CC Groningen, The Netherlands*
[4]*Institut für Biologie II, Funktionelle Proteomik, Universität Freiburg, 79104 Freiburg, Germany*
[5]*BIOSS Centre for Biological Signalling Studies, Universität Freiburg, 79104 Freiburg, Germany*

Received 2 March 2012;
received in revised form
1 May 2012;
accepted 1 May 2012
Available online
7 May 2012

Edited by J. Bowie

Keywords:
Saccharomyces cerevisiae;
Fcj1;
MINOS1;
Mio10;
SAM complex

The mitochondrial inner membrane contains a large protein complex crucial for membrane architecture, the mitochondrial inner membrane organizing system (MINOS). MINOS is required for keeping cristae membranes attached to the inner boundary membrane via crista junctions and interacts with protein complexes of the mitochondrial outer membrane. To study if outer membrane interactions and maintenance of cristae morphology are directly coupled, we generated mutant forms of mitofilin/Fcj1 (formation of crista junction protein 1), a core component of MINOS. Mitofilin consists of a transmembrane anchor in the inner membrane and intermembrane space domains, including a coiled-coil domain and a conserved C-terminal domain. Deletion of the C-terminal domain disrupted the MINOS complex and led to release of cristae membranes from the inner boundary membrane, whereas the interaction of mitofilin with the translocase of the outer membrane (TOM) and the sorting and assembly machinery (SAM) were enhanced. Deletion of the coiled-coil domain also disturbed the MINOS complex and cristae morphology; however, the interactions of mitofilin with TOM and SAM were differentially affected. Finally, deletion of both intermembrane space domains disturbed MINOS integrity as well as interactions with TOM and SAM. Thus, the intermembrane space

**Corresponding authors.* E-mail addresses: nikolaus.pfanner@biochemie.uni-freiburg.de; martin.van.der.laan@biochemie.uni-freiburg.de.

† R.M.Z. and M.B. contributed equally to this work.

Present address: K. von der Malsburg, MRC Laboratory of Molecular Biology, Cambridge, CB2 0QH, UK.

Abbreviations used: Fcj1, formation of crista junction protein 1 (mitofilin); MINOS, mitochondrial inner membrane organizing system; Mio10, Mio27, mitochondrial inner membrane organization proteins of 10 and 27 kDa, respectively; SAM, sorting and assembly machinery; TOM, translocase of outer mitochondrial membrane.

domains of mitofilin play distinct roles in interactions with outer membrane complexes and maintenance of MINOS and cristae morphology, demonstrating that MINOS contacts to TOM and SAM are not sufficient for the maintenance of inner membrane architecture.

Introduction

Mitochondria belong to the class of endosymbiotic organelles that are found in virtually all eukaryotic cells.[1] In unicellular model organisms, such as the baker's yeast *Saccharomyces cerevisiae*, mitochondria contain around 1000 different proteins, most of which are imported into the organelle upon synthesis in the cytosol.[2–6] Mitochondria form a dynamic tubular network that is dispersed throughout cells and subject to continuous rearrangements mediated by balanced fusion and fission events.[7–10] The overall morphology and ultrastructure of mitochondria is determined by the two membrane systems of these organelles, the bordering outer membrane and the inner membrane that surrounds the central matrix space.[11,12] Inner and outer mitochondrial membranes confine the intermembrane space.[13] The inner mitochondrial membrane is further divided into the inner boundary membrane that closely aligns with the outer membrane and extended tubular protrusions into the matrix termed cristae.[11,12,14] These two subdomains of the inner mitochondrial membrane show a remarkable degree of functional specialization: whereas the inner boundary membrane is, for example, enriched in protein import systems, the components of the oxidative phosphorylation machinery are preferentially found in cristae membranes.[12,15–18] Inner boundary membrane and cristae membranes are connected by morphologically well-defined membrane regions that have been named crista junctions.[11,12,19,20] Factors that have been directly or indirectly linked to the development and maintenance of the typical cristae morphology include the inner membrane fusion protein OPA1/Mgm1,[21–23] prohibitins,[24] oligomeric forms of the F_1F_o-ATP synthase,[18,25] and mitofilin.[20,26,27] The yeast mitofilin protein, also termed Fcj1 (formation of crista junction protein 1), was the first protein found to be preferentially localized to crista junction regions.[20]

Recently, a large inner membrane protein complex that consists of mitofilin/Fcj1 and at least five other subunits [Mio10 (Mcs10/Mos1), Aim5 (Mcs12), Aim13 (Mcs19), Aim37 (Mcs27), and Mio27 (Mcs29/Mos2)] was identified.[28–31] This complex was termed mitochondrial inner membrane organizing system (MINOS), mitochondrial contact site complex (MICOS), or mitochondrial organizing structure (MitOS) (nomenclatures summarized by Herrmann[32]). MINOS mutant cells exhibit a dramatically altered cristae morphology: cristae appear as large, extended stacks of lamellar membranes that are detached from the inner boundary membrane. This phenotype was shown to be most pronounced in *fcj1*Δ and *mio10*Δ mutants with an almost complete loss of crista junctions.[20,28–31] These effects on mitochondrial ultrastructure were similar to those observed upon knockdown of mitofilin in HeLa cells[26] and upon inactivation of the two *Caenorhabditis elegans* mitofilin proteins, IMMT-1 and IMMT-2.[27] Human mitofilin (IMMT, MINOS2) was found in a complex with the Mio10 ortholog MINOS1[31] and the CHCHD3 (MINOS3) protein,[31,33–35] which is related to yeast Aim13.[36] The mitochondrial morphology protein MOMA-1 identified in *C. elegans* shows homology to Aim37 and Mio27.[37] Interestingly, components of MINOS were also found to associate with a number of outer membrane protein complexes. Interaction of mitofilin/Fcj1 with the general preprotein translocase of the outer membrane (TOM complex) supports protein import via the mitochondrial intermembrane space assembly pathway.[28] Several reports identified a physical connection between mitofilin and the sorting and assembly machinery of the outer membrane (SAM complex/TOB complex),[29,31,33–35] which is required for the biogenesis of outer membrane proteins.[1,3,4] Moreover, interactions of MINOS with the outer membrane fusion protein Ugo1 and the abundant channel protein porin (VDAC) have been observed.[29,30]

It has remained unknown if and how the roles of MINOS in the formation of crista junctions and inner/outer membrane contact sites are mechanistically connected. It was suggested that the maintenance of crista junctions requires the outer membrane contacts of MINOS to connect inner boundary and cristae membranes,[29,35] pointing to a direct correlation between both MINOS functions. In this study, we have dissected yeast mitofilin/Fcj1 to define the roles of its different intermembrane space domains in outer membrane interactions and maintenance of inner membrane architecture. We show that the interactions of mitofilin with outer membrane complexes and the integrity of MINOS and inner membrane morphology are differentially affected by the deletion of mitofilin domains. The association of MINOS with the TOM and SAM complexes of the outer membrane is not sufficient for the maintenance of crista junctions.

Mutant forms of yeast mitofilin/Fcj1

Yeast mitofilin/Fcj1 consists of an N-terminal presequence required for import of the protein into mitochondria, a single transmembrane domain spanning the inner membrane and a large hydrophilic portion exposed to the intermembrane space. This intermembrane space portion contains a central putative coiled-coil domain and a C-terminal mitofilin signature domain that is highly conserved among the members of this protein family (Fig. 1a).[20,28] Protein-A-tagged wild-type Fcj1 (Fcj1-WT_{ProtA}) has been used to isolate and characterize the MINOS complex.[28] Based on this fusion protein, three mutant forms of $Fcj1_{ProtA}$ were generated (Fig. 1a): First, we removed the last 49 amino acid residues that contain the conserved C-terminal domain, generating the truncated mutant protein Fcj1-491_{ProtA}. Second, a variant lacking most of the intermembrane space portion of Fcj1 (residues 141 to 540) was produced, leading to the loss of both the coiled-coil domain and the C-terminal domain (Fcj1-140_{ProtA}). Third, an internal region of Fcj1 comprising amino acid residues 144 to 341, which includes the entire coiled-coil domain, was deleted (Fcj1-Δcc_{ProtA}). Full-length and the mutant forms of $Fcj1_{ProtA}$ were integrated into yeast chromosomal DNA to

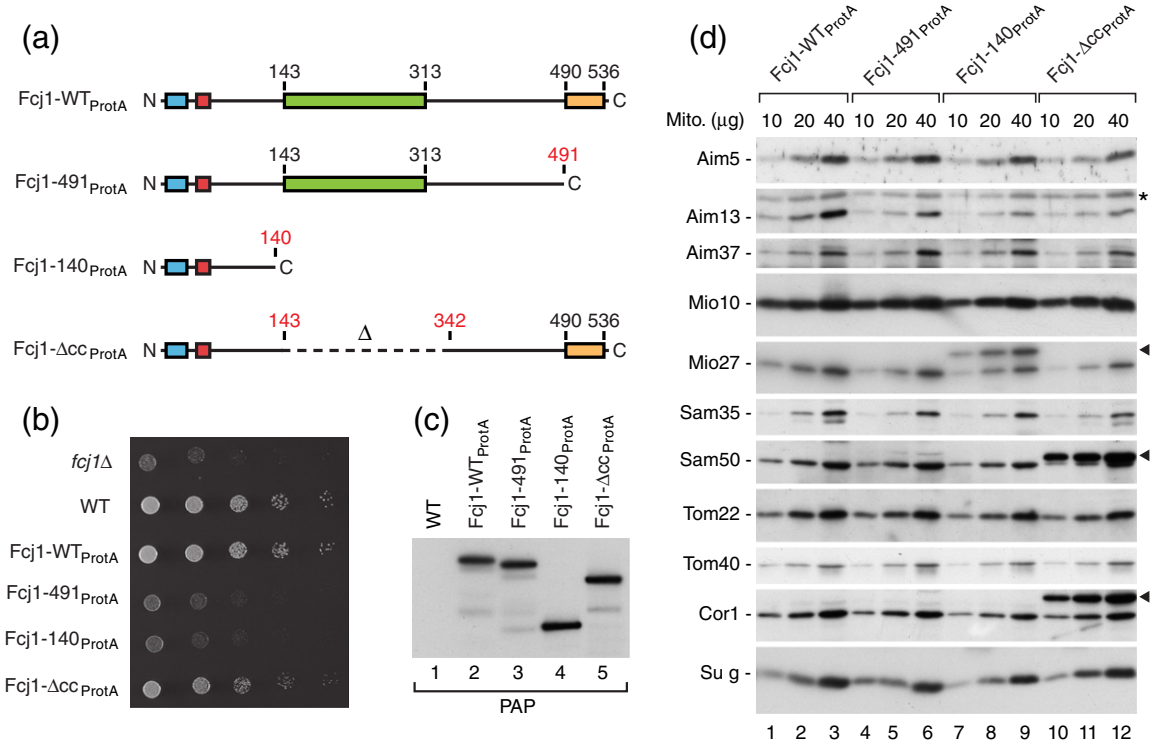

Fig. 1. Yeast mutants of mitofilin/Fcj1. (a) Schematic representation of the domain structure of wild-type (WT) mitofilin/Fcj1 (540 amino acid residues) and the domain deletion mutants used in this study. Blue, cleavable mitochondrial targeting signal (presequence); red, transmembrane segment; green, predicted coiled-coil domain (residues 143 to 313); orange; conserved C-terminal mitofilin signature domain (residues 490 to 536). All Fcj1 constructs additionally contain a C-terminal Protein A moiety. For generation of the C-terminal deletion constructs Fcj1-491_{ProtA} (lacking residues 492 to 540) and Fcj1-140_{ProtA} (lacking residues 141 to 540), a cassette comprising a Protein A affinity tag, a tobacco etch virus protease cleavage site, and a *HIS3* marker gene was integrated into the chromosome by homologous recombination, replacing the sequences that encode the indicated parts of the Fcj1 protein. The mutant *FCJ1* allele encoding Fcj1-Δcc_{ProtA} (lacking residues 144 to 341, broken line) was generated by overlap extension PCR with chromosomal DNA of a Fcj1-WT_{ProtA} strain as template. The mutant allele was integrated into the chromosomal *FCJ1* locus using a *HIS3* marker gene. (b) Growth phenotypes of the *fcj1*Δ mutant, WT yeast, and strains expressing WT Fcj1 or domain deletion mutants tagged with Protein A. Serial dilutions of cells were spotted on synthetic complete (SC) medium containing 3% (v/v) glycerol and plates were incubated at 30 °C. (c) Mitochondrial steady-state levels of $Fcj1_{ProtA}$ fusion constructs. Mitochondria were isolated from the indicated yeast strains by differential centrifugation and equal amounts of total mitochondrial proteins were separated by SDS-PAGE. Gels were blotted on polyvinylidene fluoride membranes and Protein A fusion proteins were detected using peroxidase anti-peroxidase complexes (PAP) and enhanced chemiluminescence. (d) Steady-state levels of mitochondrial proteins from yeast strains expressing Protein-A-tagged Fcj1 and Fcj1 variants as indicated. The indicated amounts of total mitochondrial proteins were analyzed as in (c). The indicated antibodies were used for immunodecoration. Su g, subunit g of F_1F_o-ATP synthase; arrowheads, signals derived from Protein A; asterisk, unspecific band.

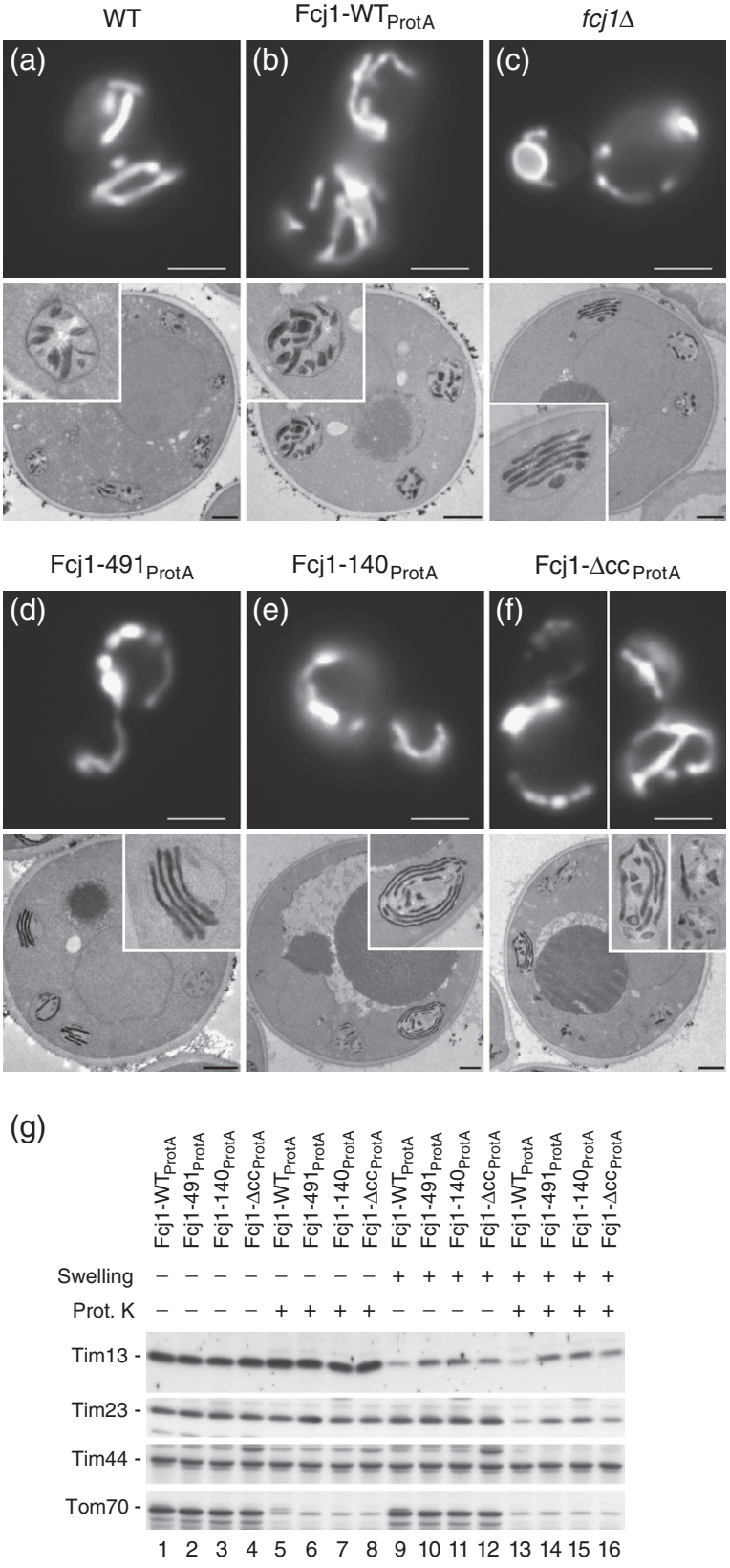

Fig. 2 (*legend on next page*)

replace the wild-type *FCJ1* gene (Fig. 1a).[28] We compared the growth behavior of Fcj1-WT_{ProtA} and the mutant forms with the different domain deletions on non-fermentable medium under conditions where the full deletion of *FCJ1* had been shown to impair yeast growth (Fig. 1b).[20,28–31] Growth of Fcj1-WT_{ProtA} cells was indistinguishable from the isogenic wild-type yeast strain expressing untagged Fcj1, confirming that the Protein A tag does not interfere with the functionality of the protein (Fig. 1b). Deletion of the C-terminal domain led to a severe growth defect comparable to the complete absence of Fcj1 (Fig. 1b, compare Fcj1-WT_{ProtA}, Fcj1-491_{ProtA}, and *fcj1*Δ). Accordingly, a similar growth defect was observed for the shortest mutant form Fcj1-140_{ProtA} lacking the C-terminal domain as well as the coiled-coil domain. In contrast, deletion of the central coiled-coil domain alone (Fcj1-Δcc_{ProtA}) only moderately impaired yeast growth (Fig. 1b). This was surprising since coiled-coil domains are generally known to mediate protein–protein interactions[38] and are therefore expected to be important for the interaction of Fcj1 with partner proteins. Taken together, the growth tests suggest that the C-terminal domain is more critical for the functionality of Fcj1 than the coiled-coil domain.

We isolated mitochondria from cells expressing Fcj1-WT_{ProtA} or one of the three mutant forms and compared the steady-state protein levels of the different Fcj1 fusion proteins by immunodetection of the Protein A moiety (Fig. 1c). The variants Fcj1-491_{ProtA}, Fcj1-140_{ProtA}, and Fcj1-Δcc_{ProtA} all accumulated in mitochondria in similar amounts compared to Fcj1-WT_{ProtA}, demonstrating that the mutant forms of Fcj1 are properly targeted and stable (Fig. 1c). We then analyzed the steady-state levels of many other proteins in wild-type and mutant mitochondria. In all Fcj1 domain deletion mitochondria, the amounts of the MINOS components Mio10 and Aim37 were comparable to wild-type (Fig. 1d). In Fcj1-Δcc_{ProtA} mitochondria, the amounts of Aim5 and Mio27 were moderately reduced (Fig. 1d, compare lanes 1–3 and 10–12). The levels of the Aim13 subunit, however, were considerably lower in each of the mutant mitochondria (Fig. 1d). This observation is consistent with the earlier finding that steady-state levels of Aim13 were dramatically reduced in *fcj1*Δ mitochondria,[28–30] indicating that the stable accumulation of Aim13 in mitochondria depends on an intact Fcj1 protein. Finally, subunits of the SAM (Sam35, Sam50) and TOM (Tom22, Tom40) complexes in the outer mitochondrial membrane and control proteins of the inner membrane (Cor1, Su g) were found in similar amounts in wild-type and all mutant mitochondria (Fig. 1d).

Altered cristae morphology in mitofilin/Fcj1 mutants

We asked how the deletion of different mitofilin/Fcj1 domains affected mitochondrial morphology and ultrastructure. A mitochondria-specific fluorescent dye was used to examine the shape of the mitochondrial network in living yeast cells. The mitochondria of wild-type and Fcj1-WT_{ProtA} cells appeared as elongated, interconnected tubules as expected, whereas *fcj1*Δ mutant mitochondria were fragmented, partially aggregated, and occasionally hollow (Fig. 2a–c).[20,28,30,31] Fcj1-491_{ProtA} and Fcj1-140_{ProtA} mitochondria looked similar to *fcj1*Δ mitochondria, whereas Fcj1-Δcc_{ProtA} mitochondria

Fig. 2. Altered cristae morphology in mitofilin/Fcj1 mutants. (a–f) Mitochondrial morphology (upper panels) and mitochondrial ultrastructure (lower panels) of the following yeast strains: wild type (WT; YPH499; 1501), Fcj1-WT_{ProtA} (2035), *fcj1*Δ (3092), Fcj1-491_{ProtA} (3380), Fcj1-140_{ProtA} (3382), and Fcj1-Δcc_{ProtA} (3387). For visualization of mitochondrial morphology, yeast cells were grown in liquid YPG medium [1% (w/v) yeast extract, 2% (w/v) bacto-peptone, 3% (v/v) glycerol] to an optical density of 0.3, pelleted by centrifugation, and resuspended in demineralized water. The mitochondria-specific fluorescent dye 3,3′-dihexyloxacarbocyanine iodide ($DiOC_6$) (100 ng/ml final concentration) was added to the cells. Small amounts of cell suspensions were applied to a glass slide coated with a mixture of 10 mM Hepes, 5% (w/v) glucose, and 1% (w/v) agarose. Mitochondrial morphology was examined with a fluorescence microscope (excitation filter band pass 470/40, emission filter band pass 525/50, dichroic mirror 495 LP), and images were recorded using a high-resolution CCD camera. Scale bars represent 5 μM. For the analysis of mitochondrial ultrastructure by electron microscopy, yeast cells were first grown in liquid medium composed of 1% (w/v) yeast extract, 2% (w/v) bacto-peptone, and 2% (v/v) L-lactate (pH 5.0) at 30 °C. This culture was then used to inoculate a minimal medium containing 2% (v/v) L-lactate (pH 5.0) supplemented with 20 mg/l amino acid mix (L-leucine, histidine, L-methionine, and uracil).[28] For staining of mitochondria with diaminobenzidine (DAB), yeast cells were fixed using 3% (v/v) glutaraldehyde in sodium cacodylate, pH 7.2, and subsequently treated with a buffer containing 0.1 M Tris–HCl (pH 7.5), 2 mg/ml DAB, and 0.06% (v/v) H_2O_2.[28] Yeast cells were post-fixed with 1.5% (w/v) $KMnO_4$, incubated overnight in 0.5% (w/v) uranylacetate, and finally embedded in Epon 812. For each strain, 100 cell sections were examined. Representative images are shown. Scale bars represent 500 nm. (g) Hypoosomotic swelling assay with mitochondria prepared from the indicated yeast cells. Isolated mitochondria (40 μg total mitochondrial proteins) in SEM buffer [250 mM sucrose, 1 mM ethylenediaminetetraacetic acid (EDTA), and 10 mM Mops/KOH, pH 7.2] were diluted 1:50 in either hypoosmotic EM buffer (1 mM EDTA and 10 mM Mops/KOH, pH 7.2) (swelling conditions)[39] or equal amounts of SEM buffer (control) and left on ice for 30 min. Mitochondria were reisolated, suspended in BSA buffer [3% (w/v) bovine serum albumin, 250 mM sucrose, 80 mM KCl, 5 mM $MgCl_2$, 2 mM KH_2PO_4, 5 mM methionine, and 10 mM Mops/KOH, pH 7.2], and treated with 50 μg/ml proteinase K (Prot. K) where indicated. Protease digestion was stopped by the addition of 2 mM PMSF. Mitochondria were washed once in SEM buffer and subjected to SDS-PAGE and immunoblotting with the indicated antisera.

showed an intermediate phenotype: Both elongated tubular segments and fragmented, condensed mitochondrial structures were observed (Fig. 2d–f). To examine the ultrastructure of mitochondria and the morphology of cristae membranes, we used diaminobenzidine staining and electron microscopy.[28] In wild-type and Fcj1-WT_{ProtA} cells, cristae membranes appeared as tubular invaginations from the inner boundary membrane with clearly defined crista junctions (Fig. 2a and b). In contrast, *fcj1*Δ cells showed an increased inner membrane surface with stacked lamellar cristae membranes and a dramatic loss of crista junctions as reported (Fig. 2c).[20,28–31] Very similar defects of mitochondrial ultrastructure were observed in Fcj1-491_{ProtA}, Fcj1-140_{ProtA}, and Fcj1-Δcc_{ProtA} yeast cells (Fig. 2d–f). In the Fcj1-Δcc_{ProtA} strain, however, these typical alterations were less pronounced: The number of cell sections with extended stacks of lamellar cristae was lower compared to the Fcj1-491_{ProtA}, Fcj1-140_{ProtA}, and *fcj1*Δ strains.

The cristae morphology defects in *fcj1*Δ mutant mitochondria have been shown to correlate with a reduced rupturing of the outer membrane under hypoosmotic conditions.[28] When isolated mitochondria are diluted into a hypoosmotic buffer, the influx of water into the organelles leads to a swelling of the matrix compartment accompanied by an unfolding of cristae and expansion of the inner boundary membrane. As the expansion capacity of the outer membrane is limited due to its smaller surface, the swelling process causes outer membrane rupture followed by the release of soluble intermembrane space proteins, like Tim13, and protease accessibility of inner membrane proteins, like Tim23 (Fig. 2g, lanes 9 and 13). This hypoosmotic swelling is impaired in *fcj1*Δ mitochondria, where the inner boundary and cristae membranes are discontinuous.[28] We tested the swelling behavior of mitochondria containing the Fcj1 truncation mutants. The release of Tim13 as well as the protease accessibility of Tim23 under hypoosmotic conditions was reduced in Fcj1-491_{ProtA}, Fcj1-140_{ProtA}, and Fcj1-Δcc_{ProtA} mitochondria compared to Fcj1-WT_{ProtA} (Fig. 2g, lanes 9–16). The swelling capacity of Fcj1-Δcc_{ProtA} mitochondria was slightly higher compared to the other two Fcj1 mutants, as judged by the slightly more efficient Tim13 release and Tim23 protease accessibility with Fcj1-Δcc_{ProtA} (Fig. 2g, lanes 10–12 and 14–16). These results are in full agreement with the differential defects in cristae morphology of the mutant mitochondria observed by electron microscopy (Fig. 2a–f).

We conclude that the deletion of either the C-terminal domain or the coiled-coil domain of mitofilin/Fcj1 has severe consequences for cristae morphology, but the defects are most pronounced, when the C-terminal domain is missing. Deletion of this conserved domain leads to morphological rearrangements of the inner membrane with the loss of crista junctions to the same extent as the complete absence of mitofilin/Fcj1, resulting in comparable growth defects of Fcj1-491_{ProtA} and *fcj1*Δ yeast strains (Fig. 1b).

Different roles of mitofilin/Fcj1 domains for MINOS integrity and outer membrane contacts

How does the deletion of different mitofilin/Fcj1 domains affect the association of Fcj1 with other MINOS components and the major outer membrane interaction partners, the TOM and SAM complexes? To address this question, we purified full-length Fcj1 and the truncated variants by affinity chromatography under mild conditions. Protein–protein contacts between different organellar membranes are particularly well preserved when whole-cell extracts are used as starting material for complex isolations.[40] To analyze both MINOS integrity and outer membrane interactions, Fcj1-WT_{ProtA}, Fcj1-491_{ProtA}, Fcj1-140_{ProtA}, and Fcj1-Δcc_{ProtA} yeast cells were cryogenically ground under liquid nitrogen. The obtained cell powder was extracted with digitonin buffer to solubilize membrane protein complexes in their native state. Fcj1-containing complexes were isolated from the detergent extracts. The MINOS subunits Mio10, Aim5, Aim13, Aim37, and Mio27 as well as the outer membrane complexes TOM (Tom22, Tom40) and SAM (Sam35, Sam50) were efficiently co-purified with Fcj1-WT_{ProtA} under these conditions, whereas control proteins of both inner membrane (Cor1, Su g) and outer membrane (Om14) were not recovered in the elution fraction (Fig. 3, lanes 8 and 11). When Fcj1-491_{ProtA} was used as bait protein, none of the MINOS subunits were co-isolated in considerable amounts, indicating that the conserved C-terminal domain of Fcj1 is of crucial importance for the integrity of MINOS (Fig. 3, lane 9). Surprisingly, co-isolation of TOM components as well as of SAM components was not impaired by the deletion of the C-terminal domain (Fig. 3, lane 9). Tom22, Tom40, Sam35, and Sam50 were detected in even higher amounts in the elution fractions of Fcj1-491_{ProtA} isolations than of Fcj1-WT_{ProtA}. These data indicate that the last 49 amino acid residues including the conserved C-terminal domain are critical for MINOS integrity but are dispensable for the association of mitofilin/Fcj1 with both SAM and TOM complexes.

We then performed affinity chromatography experiments using Fcj1-Δcc_{ProtA}. This analysis showed that the lack of the coiled-coil domain of Fcj1 leads to a partial destabilization of the MINOS complex (Fig. 3, lane 12). Whereas the

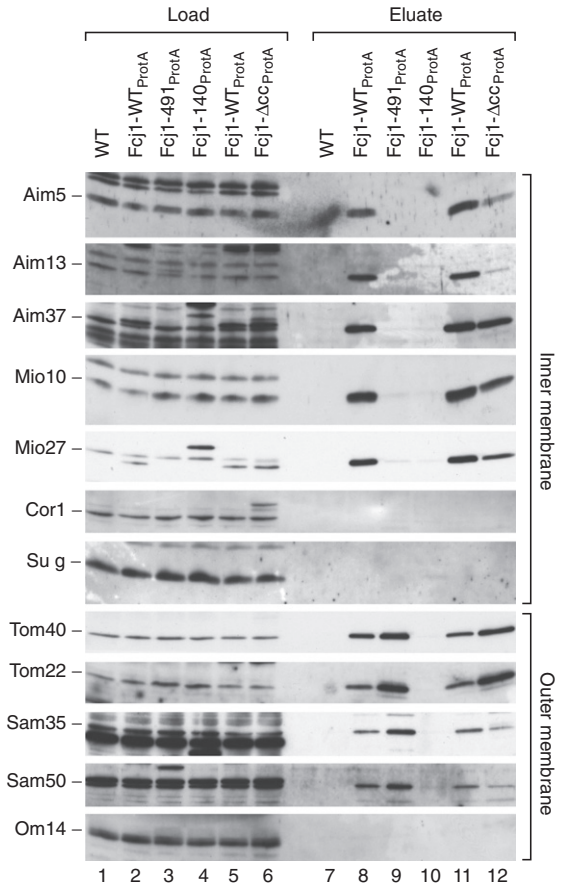

Fig. 3. Mutant forms of mitofilin/Fcj1 are differentially affected in outer membrane interactions and MINOS integrity. Yeast cells were grown in YPG medium at 30 °C, harvested by centrifugation, and washed twice with demineralized water and twice with washing buffer [20 mM Tris–HCl (pH 7.4), 50 mM NaCl, 0.1 mM ethylenediaminetetraacetic acid (EDTA), and 10% (v/v) glycerol]. Upon resuspension in washing buffer, cells were frozen in liquid nitrogen and cryogenically ground.[40] Equal amounts of cell powder derived from each of the indicated strains were extracted with digitonin buffer [20 mM Tris–HCl (pH 7.4), 50 mM NaCl, 0.1 mM EDTA, 10% (v/v) glycerol, 1% (w/v) digitonin, 2 mM PMSF, 1× Complete Protease Inhibitor Cocktail (Roche Diagnostics), and 30 μg/ml DNase I]. After a clarifying spin to remove cell debris and unsolubilized material, digitonin extracts were incubated with pre-equilibrated human immunoglobulin G-coupled Sepharose beads for 90 min at 4 °C. Beads were rinsed 15 times with washing buffer [20 mM Tris–HCl (pH 7.4), 60 mM NaCl, 0.5 mM EDTA, 10% (v/v) glycerol, 0.3% (w/v) digitonin, and 2 mM PMSF] to remove unbound material. Bound proteins were eluted by cleavage with tobacco etch virus protease. Samples were analyzed by SDS-PAGE and Western blotting with the indicated antisera. Load, 1.5%; eluate, 100%. Su g, subunit g of F_1F_o-ATP synthase.

association of Aim5 and Aim13 with Fcj1-Δcc_{ProtA} was strongly impaired compared to Fcj1-WT_{ProtA}, the co-isolation of Aim37, Mio10, and Mio27 was only moderately affected. For the interaction of Fcj1-Δcc_{ProtA} with the TOM and SAM complexes, we obtained differential results. The co-purification of the TOM subunits Tom22 and Tom40 was increased upon removal of the coiled-coil domain, similar to the situation with the C-terminal domain deletion mutant (Fig. 3, lane 12 compared to lane 9). The recovery of Sam35 and Sam50 with Fcj1-Δcc_{ProtA}, however, was considerably reduced in comparison to Fcj1-WT_{ProtA} (Fig. 3, lanes 11 and 12). Finally, the lack of both coiled-coil and C-terminal domain in the Fcj1-140_{ProtA} construct led to a loss of both MINOS integrity and interaction with the TOM and SAM complexes (Fig. 3, lane 10).

In conclusion, our data demonstrate that distinct domains of mitofilin/Fcj1 differentially contribute to MINOS integrity and cristae morphology on the one hand and interaction with the outer membrane complexes TOM and SAM on the other hand. The conserved C-terminal signature domain of mitofilin/Fcj1 is critical for the stability of the MINOS complex, maintenance of cristae morphology, and yeast growth, but not for the formation of inner/outer membrane contacts through the TOM and SAM complexes. The coiled-coil and C-terminal domains differentially contribute to the association of mitofilin/Fcj1 with the TOM and SAM complexes. We show that the interaction of mitofilin/Fcj1 with TOM and SAM is not sufficient to preserve the connections between inner boundary membrane and cristae membranes in the absence of assembled MINOS complexes. These findings suggest that the functions of MINOS for cristae maintenance and formation of membrane contact sites can be dissected and thus involve distinct mechanisms. It has been proposed that MINOS, TOM, and SAM are integrated in a large endoplasmic reticulum–mitochondria organizing network (ERMIONE), which plays crucial roles in mitochondrial biogenesis and membrane architecture.[41] The dissection of distinct MINOS functions reported here supports the view that ERMIONE is a dynamic system and provides a basis for a mechanistic analysis of this organizing network.

Acknowledgements

This work was supported by the Deutsche Forschungsgemeinschaft, Sonderforschungsbereich 746, Excellence Initiative of the German Federal and State Governments (EXC 294 BIOSS; GSC-4 Spemann Graduate School), Landesforschungspreis

Baden-Württemberg, Gottfried Wilhelm Leibniz Program, and Bundesministerium für Bildung und Forschung.

References

1. Dolezal, P., Likic, V., Tachezy, J. & Lithgow, T. (2006). Evolution of the molecular machines for protein import into mitochondria. *Science*, **313**, 314–318.
2. Baker, M. J., Frazier, A. E., Gulbis, J. M. & Ryan, M. T. (2007). Mitochondrial protein-import machinery: correlating structure with function. *Trends Cell Biol.* **17**, 456–464.
3. Neupert, W. & Herrmann, J. M. (2007). Translocation of proteins into mitochondria. *Annu. Rev. Biochem.* **76**, 723–749.
4. Chacinska, A., Koehler, C. M., Milenkovic, D., Lithgow, T. & Pfanner, N. (2009). Importing mitochondrial proteins: machineries and mechanisms. *Cell*, **138**, 628–644.
5. Endo, T., Yamano, K. & Kawano, S. (2011). Structural insight into the mitochondrial protein import system. *Biochim. Biophys. Acta*, **1808**, 955–970.
6. Schmidt, O., Pfanner, N. & Meisinger, C. (2010). Mitochondrial protein import: from proteomics to functional mechanisms. *Nat. Rev., Mol. Cell Biol.* **11**, 655–667.
7. Okamoto, K. & Shaw, J. M. (2005). Mitochondrial morphology and dynamics in yeast and multicellular eukaryotes. *Annu. Rev. Genet.* **39**, 503–536.
8. Hoppins, S., Lackner, L. & Nunnari, J. (2007). The machines that divide and fuse mitochondria. *Annu. Rev. Biochem.* **76**, 751–780.
9. Campello, S. & Scorrano, L. (2010). Mitochondrial shape changes: orchestrating cell pathophysiology. *EMBO Rep.* **11**, 678–684.
10. Westermann, B. (2010). Mitochondrial fusion and fission in cell life and death. *Nat. Rev., Mol. Cell Biol.* **11**, 872–884.
11. Mannella, C. A. (2006). The relevance of mitochondrial membrane topology to mitochondrial function. *Biochim. Biophys. Acta*, **1762**, 140–147.
12. Zick, M., Rabl, R. & Reichert, A. S. (2009). Cristae formation—linking ultrastructure and function of mitochondria. *Biochim. Biophys. Acta*, **1793**, 5–19.
13. Herrmann, J. M. & Riemer, J. (2010). The intermembrane space of mitochondria. *Antioxid. Redox Signal.* **13**, 1341–1358.
14. Osman, C., Merkwirth, C. & Langer, T. (2009). Prohibitins and the functional compartmentalization of mitochondrial membranes. *J. Cell Sci.* **122**, 3823–3830.
15. Gilkerson, R. W., Selker, J. M. & Capaldi, R. A. (2003). The cristal membrane of mitochondria is the principal site of oxidative phosphorylation. *FEBS Lett.* **546**, 355–358.
16. Vogel, F., Bornhövd, C., Neupert, W. & Reichert, A. S. (2006). Dynamic subcompartmentalization of the mitochondrial inner membrane. *J. Cell Biol.* **175**, 237–247.
17. Wurm, C. A. & Jakobs, S. (2006). Differential protein distributions define two sub-compartments of the mitochondrial inner membrane in yeast. *FEBS Lett.* **580**, 5628–5634.
18. Strauss, M., Hofhaus, G., Schröder, R. R. & Kühlbrandt, W. (2008). Dimer ribbons of ATP synthase shape the inner mitochondrial membrane. *EMBO J.* **27**, 1154–1160.
19. Renken, C., Siragusa, G., Perkins, G., Washington, L., Nulton, J., Salamon, P. & Frey, T. G. (2002). A thermodynamic model describing the nature of the crista junction: a structural motif in the mitochondrion. *J. Struct. Biol.* **138**, 137–144.
20. Rabl, R., Soubannier, V., Scholz, R., Vogel, F., Mendl, N., Vasiljev-Neumeyer, A. *et al.* (2009). Formation of cristae and crista junctions in mitochondria depends on antagonism between Fcj1 and Su *e/g*. *J. Cell Biol.* **185**, 1047–1063.
21. Olichon, A., Baricault, L., Gas, N., Guillou, E., Valette, A., Belenguer, P. & Lenaers, G. (2003). Loss of OPA1 perturbates the mitochondrial inner membrane structure and integrity, leading to cytochrome *c* release and apoptosis. *J. Biol. Chem.* **278**, 7743–7746.
22. Frezza, C., Cipolat, S., Martins de Brito, O., Micaroni, M., Beznoussenko, G. V., Rudka, T. *et al.* (2006). OPA1 controls apoptotic cristae remodeling independently from mitochondrial fusion. *Cell*, **126**, 177–189.
23. Meeusen, S., DeVay, R., Block, J., Cassidy-Stone, A., Wayson, S., McCaffery, J. M. & Nunnari, J. (2006). Mitochondrial inner-membrane fusion and crista maintenance requires the dynamin-related GTPase Mgm1. *Cell*, **127**, 383–395.
24. Merkwirth, C., Dargazanli, S., Tatsuta, T., Geimer, S., Löwer, B., Wunderlich, F. T. *et al.* (2008). Prohibitins control cell proliferation and apoptosis by regulating OPA1-dependent cristae morphogenesis in mitochondria. *Genes Dev.* **22**, 476–488.
25. Paumard, P., Vaillier, J., Coulary, B., Schaeffer, J., Soubannier, V., Mueller, D. M. *et al.* (2002). The ATP synthase is involved in generating mitochondrial cristae morphology. *EMBO J.* **21**, 221–230.
26. John, G. B., Shang, Y., Li, L., Renken, C., Mannella, C. A., Selker, J. M. *et al.* (2005). The mitochondrial inner membrane protein mitofilin controls cristae morphology. *Mol. Biol. Cell*, **16**, 1543–1554.
27. Mun, J. Y., Lee, T. H., Kim, J. H., Yoo, B. H., Bahk, Y. Y., Koo, H. S. & Han, S. S. (2010). *Caenorhabditis elegans* mitofilin homologs control the morphology of mitochondrial cristae and influence reproduction and physiology. *J. Cell. Physiol.* **224**, 748–756.
28. von der Malsburg, K., Müller, J. M., Bohnert, M., Oeljeklaus, S., Kwiatkowska, P., Becker, T. *et al.* (2011). Dual role of mitofilin in mitochondrial membrane organization and protein biogenesis. *Dev. Cell*, **21**, 694–707.
29. Harner, M., Körner, C., Walther, D., Mokranjac, D., Kaesmacher, J., Welsch, U. *et al.* (2011). The mitochondrial contact site complex, a determinant of mitochondrial architecture. *EMBO J.* **30**, 4356–4370.
30. Hoppins, S., Collins, S. R., Cassidy-Stone, A., Hummel, E., DeVay, R. M., Lackner, L. L. *et al.* (2011). A mitochondrial-focused genetic interaction map reveals a scaffold-like complex required for inner membrane organization in mitochondria. *J. Cell Biol.* **195**, 323–340.
31. Alkhaja, A. K., Jans, D. C., Nikolov, M., Vukotic, M., Lytovchenko, O., Ludewig, F. *et al.* (2012). MINOS1 is a conserved component of mitofilin complexes and

required for mitochondrial function and cristae organization. *Mol. Biol. Cell*, **23**, 247–257.
32. Herrmann, J. M. (2011). MINOS is plus: a Mitofilin complex for mitochondrial membrane contacts. *Dev. Cell*, **21**, 599–600.
33. Xie, J., Marusich, M. F., Souda, P., Whitelegge, J. & Capaldi, R. A. (2007). The mitochondrial inner membrane protein mitofilin exists as a complex with SAM50, metaxins 1 and 2, coiled-coil-helix coiled-coil-helix domain-containing protein 3 and 6 and DnaJC11. *FEBS Lett.* **581**, 3545–3549.
34. Darshi, M., Mendiola, V. L., Mackey, M. R., Murphy, A. N., Koller, A., Perkins, G. A. *et al.* (2011). ChChd3, an inner mitochondrial membrane protein, is essential for maintaining crista integrity and mitochondrial function. *J. Biol. Chem.* **286**, 2918–2932.
35. Ott, C., Ross, K., Straub, B., Thiede, B., Götz, M., Goosmann, C. *et al.* (2012). Sam50 functions in mitochondrial intermembrane space bridging and biogenesis of respiratory complexes. *Mol. Cell. Biol.* **32**, 1173–1188.
36. Cavallaro, G. (2010). Genome-wide analysis of eukaryotic twin CX_9C proteins. *Mol. BioSyst.* **6**, 2459–2470.
37. Head, B. P., Zulaika, M., Ryazantsev, S. & van der Bliek, A. M. (2011). A novel mitochondrial outer membrane protein, MOMA-1, that affects cristae morphology in *Caenorhabditis elegans*. *Mol. Biol. Cell*, **22**, 831–841.
38. Grigoryan, G. & Keating, A. E. (2008). Structural specificity in coiled-coil interactions. *Curr. Opin. Struct. Biol.* **18**, 477–483.
39. Stojanovski, D., Pfanner, N. & Wiedemann, N. (2007). Import of proteins into mitochondria. *Methods Cell Biol.* **80**, 783–806.
40. Stroud, D. A., Oeljeklaus, S., Wiese, S., Bohnert, M., Lewandrowski, U., Sickmann, A. *et al.* (2011). Composition and topology of the endoplasmic reticulum-mitochondria encounter structure. *J. Mol. Biol.* **413**, 743–750.
41. van der Laan, M., Bohnert, M., Wiedemann, N. & Pfanner, N. (2012). Role of MINOS in mitochondrial membrane architecture and biogenesis. *Trends Cell Biol.* **22**, 185–192.